Pharmaceutical Research, Vol. 24, No. 2, February 2007 (© 2006)
DOI: 10.1007/s11095-006-9154-7

Research Paper

Preparation and Characterization of Nickel Nanoparticles for Binding to His-tag Proteins and Antigens

Jigna D. Patel,[1] Ronan O'Carra,[1] Julia Jones,[2] Jerold G. Woodward,[2] and Russell J. Mumper[1,3]

Received May 23, 2006; accepted August 28, 2006; published online December 19, 2006

Purpose. The purpose of these studies was to prepare nanoparticles (NPs) with a small amount of surface-chelated nickel for obtaining enhanced binding of histidine-tagged (his-tag) proteins compared to non-histidine-tagged protein binding to charged nanoparticles.
Materials and Methods. NPs were prepared from oil-in-water microemulsion precursors using emulsifying wax, 3 mM Brij 78 and 0.1 mM DOGS–NTA–Ni lipid (referred to as Ni-NPs). The amount of lipid entrapped in the NPs was quantitated by atomic emission spectroscopy (AES). The Ni-NPs were investigated for binding to two his-tag proteins, green fluorescent protein (GFP) and his-tag HIV-1 Gag p24. *In vivo* studies in mice were carried out to evaluate the immune responses obtained to his-tag Gag p24 bound to Ni-NPs.
Results. AES studies demonstrated that approximately 5% of the DOGS–NTA–Ni lipid used was entrapped in the NPs. The optimal binding ratio his-tag GFP and his-tag Gag p24 to Ni-NPs was found to be 1:33.7 and 1:35.4 w/w, respectively. This interaction was stable at 37°C in PBS, pH 7.4 over 4 h and the interaction of his-tag GFP with the Ni-NPs was enhanced compared to control NPs prepared with no Ni on the surface (NTA-NPs). The *in vivo* studies demonstrated enhanced serum IgG and IgG2a responses to his-tag Gag p24 bound to Ni-NPs compared to protein adjuvanted with Alum or adsorbed on the surface of control NTA-NPs.
Conclusions. Ni-NPs can be used to bind strongly to his-tag proteins. This system was demonstrated to have potential applications in vaccine delivery for enhancing immune responses to protein-based vaccines.

KEY WORDS: nanoparticles; nickel; histidine tagged proteins; HIV-1 Gag p24.

INTRODUCTION

The need for improved adjuvants for enhancing immune responses to protein-based vaccines is widely recognized (1–3). Presently, Alum continues to be the only approved adjuvant for routine human vaccination in the US (1). However, there has been considerable interest in the development of particulate delivery systems for enhancing immune responses with protein-based vaccines over the past few years (4–6). Particulate delivery systems are attractive as they offer numerous advantages such as the ability to (1) control the release of the antigen (7,8), (2) target the delivery of antigen to antigen presenting cells (APCs) (9,10), and (3) incorporate immunostimulatory adjuvants for synergistic enhancements in immune responses (11,12). Moreover, particulate delivery systems are of similar sizes as naturally occurring pathogens and considered to be rapidly taken up by APCs, leading to increased accumulation of the associated protein inside the cell (13).

Particulate delivery systems for protein-based vaccine applications have most often utilized entrapment of the antigen within the particle for obtaining enhanced immune responses (4,14,15). Although effective, concerns associated with this approach include protein instability and entrapment efficiency. For example, the protein stability is of significant concern with the most often investigated PLGA microparticles (16). The protein degradation can occur during the entrapment due to exposure to organic solvents, during freeze drying, and also by the acidic environment created by polymer degradation *in vivo* (17). Moreover, low entrapment of the protein and instability of the delivery system are challenges faced with using liposomal systems. Alternatively, the use of charged particles has been investigated for coating antigens to the particle surface by charge interaction and thus, enhancing immune responses to the coated antigen *in vivo* (16,18,19). To this end, reports from our laboratory have demonstrated the potential of charged nanoparticles (NPs) prepared from oil-in-water microemulsion precursors for enhancing immune responses with cationic proteins such as β-galactosidase (20) and HIV-1 Tat protein (21,22).

Several studies suggest that the higher uptake of antigens into APCs by using particulate delivery systems play a

[1] Department of Pharmaceutical Sciences, College of Pharmacy, University of Kentucky, Lexington, KY 40536-0082, USA.
[2] Department of Microbiology, Immunology and Molecular Genetics, University of Kentucky, Lexington, KY 40536-0298, USA.
[3] To whom correspondence should be addressed. (e-mail: rjmump2@email.uky.edu)

vital role in enhancing the immune response to associated antigens *in vivo* (23–25). Studies in our laboratory have demonstrated that NPs are taken up effectively *in vitro* by DCs and that the enhanced delivery of associated antigen or molecules, at least in part, contributes to the enhanced immune responses observed *in vivo* (unpublished data). These are antigens simply coated on charged particles and it is possible that some dissociation of the coated protein from the particle may occur *in vivo* due to presence of other charged molecules, resulting in a decreased accumulation in APCs. Thus, it is hypothesized that increasing the interaction of the antigen for the particles could lead to increased accumulation of the antigen in the APCs as compared to antigen coated on the surface of charged NPs and thus, enabling greater enhancements in immune responses *in vivo*.

The attachment of proteins and antibodies to particulate delivery systems has been investigated extensively by covalent linkages that involve the use of sulfhydryl-, amine- and carboxyl-reactive moieties on the protein or the particle (26–28). However, these approaches are often cumbersome and require the use of activating or reducing agents. In addition, these methods have the potential for causing protein degradation during attachment, random or multiple point attachment of the protein, and quite often, low coupling efficiencies are obtained. An alternative approach taking advantage of affinity interactions has been extensively used for purification of recombinant proteins (29,30). This approach exploits the interaction between chelated divalent metal ions such as nickel, copper, or cobalt and a short sequence of histidine residues (four to ten repeating units) added to the N- or C-terminus of the protein, referred to as histidine-tags (his-tag). These purification methods generally involve immobilizing the metal ion onto the column packing material using a chelating agent such as nitrilotriacetic acid (NTA) (29). In the case of Cu^{2+} and Ni^{2+} which have six coordination sites, NTA forms a strong complex with four of the metal sites, leaving two additional sites for interaction with the his-tag present on the protein (31). Moreover, the interaction of his-tags with NTA–Ni has been reported to be stronger than or equivalent to that of antibody interactions (10^{-6} to 10^{-9}M), with a dissociation constants (K_d) in the range of 10^{-6} to 10^{-13} M at pH 7–8 depending on the protein and location of the his-tag on the protein (32,33). The binding is reversible by competing off with excess imidazole (>100 mM) or by lowering the pH, which results in release of the his-tag protein due to protonation of electron donating histidine groups (p*K*a=6.0). In addition to its extensive use in protein purification, the use of NTA–Ni has been also reported for immobilization of his-tag proteins onto surfaces for structural and functional studies (34) and for studying protein interactions by flow cytometry (33). More recently, hydrophobized NTA–Ni ligand integrated in the liposomal lipid bilayer was reported for attaching his-tag peptides and proteins on the surface (35) and for targeting the uptake of entrapped antigen to DCs via surface immobilization of his-tag antibodies for DC-specific receptors (36).

The interaction of chelated Ni with his-tag proteins for enhancing immune responses to antigens with particulate delivery systems would be advantageous since it is simple, applicable to a wide range of proteins, and offers stronger interactions between the particle and antigen compared to conventional charged particles, consequently allowing for higher accumulation of antigen into the cell. Once the antigen is taken up into the cells, it can also be released because the interactions weaken in the acidic environment of the lysosomes. Therefore, the present studies were aimed at investigating the preparation of NPs with a small amount of surface-chelated nickel for binding to his-tag proteins. In addition, the utility of these NPs for enhancing the immune responses to protein-based vaccines was evaluated *in vivo* using his-tag HIV-1 Gag p24 protein.

The HIV gag gene encodes for four major Gag proteins in the mature virus (37) and the Gag proteins are currently under investigation as potential candidates for the HIV vaccines (http://www.iavireport.org/trialsdb/). Of these four proteins, the Gag p24 protein has been shown to be the most conserved among the different HIV subtypes (38) and many groups have also identified Gag p24 as the target of Gag-specific cellular responses (38–40). More importantly, a recent study of HIV-infected patients highlighted the significance of strong Gag p24-specific cellular responses in controlling viral replication and $CD4^+$ T cell counts (41). Thus, these features made the HIV-1 Gag p24 protein an attractive and relevant choice for further evaluating immune responses *in vivo* with the nickel nanoparticles.

MATERIALS AND METHODS

Materials

Emulsifying wax, comprised of cetyl alcohol and polysorbate 60 (molar ratio of 20:1) and Alum were purchased from Spectrum (New Brunswick, NJ). Phosphate buffered saline, pH 7.4 (PBS), PBS, pH 7.4 with 0.05% Tween 20 (PBS/Tween 20), bovine serum albumin (BSA), and Sepharose CL4B were from Sigma Chemical Co. (St. Louis, MO). Brij 78 was purchased from Uniqema (New Castle, DE). Sheep anti-mouse IgG, peroxidase-linked species specific $F(ab')_2$ fragment was purchased from Amersham Pharmacia Biotech (Piscataway, NJ). IFN-γ ELISA kit, streptavidin–horseradish peroxidase (Sv–HRP) and biotinylated rat anti-mouse IgG1 and IgG2a monoclonal antibodies were from BD Biosciences Pharmingen (San Diego, CA). Tetramethylbenzidine (TMB) substrate kit and HisGrab™ nickel coated plates were purchased from Pierce (Rockford, IL). Microcon® YM-100, CentriPlus® YM-100, 2-mercaptoethanol, certified nickel standard (Claritas® certified reference material) and nitric acid (trace metal grade) were purchased from Fisher Scientific (Hampton, NH). RPMI 1640, 10% heat-inactivated FBS, HEPES, L-glutamine, penicillin, and streptomycin were from GIBCO (Carlsband, CA). His-tag GFP was purchased from Upstate (Charlottesville, VA). His-tag HIV-1 Gag p24 (his-tag p24) was obtained through the Centralised Facility for AIDS Reagents supported by EU Programme EVA/MRC and the UK Medical Research Council (donated by Dr. I. Jones). 1,2-Dioleoyl-*sn*-Glycero-3-[(*N*-(5-amino-1-carboxypentyl)iminodiacetic acid)succinyl] nickel and ammonium salt, abbreviated DOGS–NTA–Ni and DOGS–NTA, respectively, were purchased from Avanti Polar Lipids (Alabastar, AL). Polyvinylidene fluoride (PVDF) membranes, 15% Tris-Hydrochloride (Tris-HCl) SDS-PAGE gels, and Immun-star HRP substrate kit were

from Bio-Rad (Hercules, CA). For *in vivo* studies, female BALB/c mice (6–8 weeks old) were obtained from Harlan Sprague–Dawley Laboratories (Indianapolis, IN).

Preparation of NPs with Surface-Chelated Ni

In a 7 ml glass vial, 2 mg of emulsifying wax (the oil phase) and 3.5 mg (3 mM) of Brij 78 (the surfactant) were added and then melted at 60–65°C. To this vial, 10.6 μl (0.1 mM) of DOGS–NTA–Ni (10 mg/ml stock in chloroform) was added and the chloroform was evaporated on a hot plate (~60–65°C) while stirring. De-ionized, 0.2 micron-filtered water (1,000 μl) was added to the vial at 60–65°C and the contents of the vial were mixed on the hot plate to form clear oil-in-water microemulsions. NPs were obtained by cooling the vials to room temperature while stirring. NPs of similar composition but without Ni were prepared in the same manner using 0.1 mM of DOGS–NTA lipid instead, referred to as NTA-NPs. The NPs were characterized by measuring their size using a Coulter N4 Plus Sub-Micron Particle Sizer (Coulter Corporation, Miami, FL) at 90° and charge, using a Malvern Zeta Sizer 2000 (Malvern Instruments, Southborough, MA).

Binding of His-tag p24 and Initial *In Vivo* Studies

For the initial studies, his-tag p24 was bound to the surface-chelated Ni nanoparticles (Ni-NPs) at a 1:10 w/w ratio (dry weight ratio of protein to Ni-NPs) in PBS, pH 7.4 at 4°C overnight. The effectiveness of these formulations with respect to Alum and NTA-NPs was evaluated *in vivo*. These control formulations were prepared by simply mixing the appropriate amount of his-tag p24 with Alum or NTA-NPs in PBS, pH 7.4 for at least 1 h at room temperature. The mice (n=5–6 per group) were dosed on day 0 and 14 with his-tag p24 bound to Ni-NPs, adjuvanted with Alum, or as a control coated on NTA-NPs. All mice were given 100 μl s.c. injections on the back containing 2.5 μg of his-tag p24 and 25 μg of the NPs or Alum. The mice were bled by cardiac puncture on day 28 and the sera were separated and stored at −20°C for antigen-specific IgG analysis.

Determination of His-tag p24-Specific Total IgG Levels

His-tag p24-specific serum IgG levels were determined using an ELISA. The wells (96-well Costar plates) were coated with 50 μl of his-tag p24 (5 μg/ml in PBS, pH 7.4) overnight at 4°C. The plates were blocked for 1 h at 37°C with 200 μl of 4% BSA prepared in PBS/Tween 20. The plates were then incubated with 50 μl per well of mouse serum diluted at 1:100 and 1:1,000 in 4%BSA/PBS/Tween 20 for 2 h at 37°C. The plates were incubated with 50 μl/well anti-mouse IgG HRP $F(ab')_2$ fragment from sheep (1:3,000 in 1%BSA/PBS/Tween 20) for 1 h at 37°C. The plates were washed three to five times with PBS/Tween 20 in between each step. The plates were developed by adding 100 μl of TMB substrate and incubating for 30 min at RT. The color development was stopped by the addition of 100 μl of 2M H_2SO_4 and the OD at 450 nm was read using a Universal Microplate Reader (Bio-Tek Instruments, Inc., Winooski, VT).

Optimization of Ni-NP Formulation for Binding to His-tag Proteins Using His-tag GFP

Studies evaluating the entrapment and binding ratios of Ni-NPs to a model protein, his-tag GFP, were carried out. Excess DOGS–NTA–Ni was separated from the Ni-NPs by using a gravity packed Sepharose CL4B gel permeation chromatography (GPC) column (15×70 mm). Briefly, 200 μl of the Ni-NPs was passed down the GPC column using PBS, pH 7.4 as the mobile phase. Fractions (1 ml) were collected and the fractions containing the NPs (as determined by measuring the particle size intensity with the particle sizer) were used for binding to his-tag GFP. To determine the optimal binding ratios, his-tag GFP was mixed with the GPC-purified Ni-NPs at a 1:16.9 and 1:33.7 w/w ratios in PBS, pH 7.4 at 4°C overnight. Free protein was separated from bound protein by passing through the Sepharose CL4B column using PBS, pH 7.4 as the mobile phase. Fractions collected (1 ml) were analyzed by fluorescence to determine the percent of his-tag GFP bound to Ni-NPs. The stability of the binding at 1:33.7 w/w ratio at 37°C in PBS, pH 7.4 was evaluated by removing aliquots at over 4 h and passing through the GPC column. The fluorescence associated in fraction 1–12 was measured, and particle sizes were measured using fraction 4. The fluorescence was measured using a Hitachi F-2000 fluorescence spectrophotometer (Fairfield, OH) with excitation and emission wavelengths set at 395 and 508 nm, respectively.

Optimization of His-tag p24 Binding to Ni-NPs

The Ni-NPs were purified by GPC as described and further bound to the his-tag p24 at 1:8.85, 1:17.7, 1:35.4, and 1:70.8 w/w ratios to determine the optimal binding conditions. After GPC purification, fractions 7–13 were evaluated for the presence of free protein by ELISA. The NP containing fractions, 3–5, were combined, concentrated using Microcon® YM-100 ultracentrifuge devices, and analyzed by Western blot.

ELISA for Analysis of Free His-tag p24

To detect the free his-tag p24 eluting from GPC column, a qualitative ELISA method was developed using HisGrab™ nickel-coated plates. Samples (100 μl) were added to the plate and incubated for 1 h at room temperature (RT) while shaking. The wells were blocked with 200 μl of 1% fetal bovine serum (heat inactivated) in PBS/Tween 20 for 1 h at RT. His-tag p24 anti-sera (from the initial studies) diluted at 1:1,000 in blocking solution was added to the wells (100 μl) and incubated for 1 h at RT. Finally, 100 μl of anti-mouse IgG HRP $F(ab')_2$ fragment from sheep diluted at 1:3,000 in the blocking solution was added and the plate was incubated for 1 h at RT. The plates were washed three to five times with PBS/Tween 20 in between each step. The plates were developed by incubating with 100 μl of TMB substrate 30 min at RT and the color development was stopped by the addition of 100 μl of 2 M H_2SO_4. The OD at 450 nm was measured using a plate reader.

Western Blot Analysis for His-tag p24 Bound to Ni-NPs

The concentrated NP fractions after GPC purification along with various amounts of his-tag p24 as controls were loaded on 15% Tris-HCl SDS-PAGE gels using Bio-rad power supply (200 V constant for 45 min). A semi-dry transfer of the proteins from the SDS-PAGE gel onto a PVDF membrane was performed using Trans-Blot semi dry transfer cell (Bio-rad) using the Bio-rad power supply (15 V, 120 mA, 400 W for 24 min). The membrane was blocked for 1 h with 4% BSA prepared in PBS/Tween 20 and then incubated with a 1:1,000 dilution of his-tag p24 anti-sera from the initial experiment for 2 h. Finally, the membrane was incubated with a 1:5,000 anti-mouse IgG HRP $F(ab')_2$ fragment from sheep for 1 h. All antibodies were diluted in 4% BSA in PBS/Tween 20. All steps were performed with shaking at RT and three to five washings for 5 min using PBS/Tween 20 were included in between each step. The protein on the membrane was detected using the Immun-star HRP substrate kit and the membrane was exposed using a Kodak Image Station 2,000 mm (New Haven, CT) and analyzed using Kodak 1D software.

Atomic Emission Spectroscopy for Quantitating the Surface-chelated Ni on NPs

Atomic emission spectroscopy (AES) using inductively coupled plasma as the excitation source was used to quantify Ni present on the Ni-NPs before and after GPC purification. The method parameters set on the Varian Vista-PRO CCD simultaneous ICP-OES instrument (Palo Alto, CA) were as follows: plasma flow at 15.0 l/min; auxiliary flow at 1.50 l/min; nebulizer flow at 0.90 ml/min; sample uptake 30 s; rinse time 10 s; and pump rate 15 rpm. Yttrium was used as an internal standard for correction as needed. The Ni was detected at 216.55 and 231.604 nm and the final results were calculated based on an average of both wavelengths. The data was collected and analyzed by Vista-PRO ICP software v.4.1.0. All samples and standards were prepared using 5% nitric acid. A standard curve for Ni was prepared from 10 to 200 ppb Ni. For quality control purposes, independent Ni standards at 20 and 100 ppb were prepared and analyzed prior to sample analysis. The acceptance criteria for the quality control standards were based on greater 90% of theoretical Ni concentration. To determine the recovery of Ni from the NP matrix, 0.4 and 2.0 mg of NTA-NPs were spiked with 10 and 50 ppb of Ni and analyzed for Ni content. For quantitation of Ni on the Ni-NPs, the NPs were purified by GPC to obtain a total of 2.0 mg of purified NPs and fractions 3–6 were collected. The combined fractions were further desalted and concentrated using CentriPlus® YM-100 ultracentrifuge devices to a final volume of 1 ml and diluted in nitric acid for analysis.

In Vitro Release of His-tag p24 from Ni-NPs as a Function of pH

His-tag p24 was bound to purified Ni-NPs at a ratio of 1:70.8 w/w as described above. After GPC purification, the NP containing fractions were combined and concentrated using Microcon® YM-100 ultracentrifuge devices. Aliquots of the Ni-NPs, with bound his-tag p24, were incubated under increasing acidic conditions; pH 7.4 (Control), pH 6.2, pH 5.0 and pH 4.0. The release study at pH 7.4 and pH 6.2 was performed using 10 and 50 mM phosphate buffer, respectively. The release study at pH 5.0 and pH 4.0 was performed using 50 mM acetate buffer. The osmolality of all buffer systems was maintained at 300 mOsm/kg with NaCl. After 1 h incubation at 25°C, the Ni-NPs were applied to a GPC column equilibrated with a mobile phase of appropriate pH e.g., samples incubated at pH 5.0 were eluted by acetate buffer with a pH of 5.0. The NP containing fractions were combined, concentrated and analyzed by Western blot as described above. The relative amount of his-tag p24 retained on the Ni-NPs was determined by calculating the band intensities and comparing it to that of the control (pH 7.4) using Kodak 1D software analysis.

In Vivo Assessment of Optimized HIV-1 His-tag p24 Bound to Ni-NPs

Mice (n=6–8 per group) were immunized (s.c.) on day 0 and 14 with 100 μl of his-tag p24 bound to GPC purified Ni-NPs, coated on NTA-NPs, or adjuvanted with Alum. As an additional control, his-tag p24 bound to unpurified Ni-NPs were also assessed. The dose of his-tag p24 was 2.5 μg and of the NPs or Alum was 88.5 μg. On day 28, mice were bled by cardiac puncture, and the sera were collected and stored at −20°C for IgG analysis. The spleens were collected and pooled for each group for splenocyte proliferation and IFN-γ release assays.

His-tag p24-specific Antibody Isotype Analysis

His-tag p24 specific IgG1 and IgG2a levels were determined using an ELISA procedure similar to that described for total IgG levels. Briefly, the plates were coated with 50 μl of his-tag p24 (1 μg/ml in PBS, pH 7.4) overnight at 4°C. The plates were blocked with 4% BSA in PBS/Tween 20 for 1 h at 37°C. The sera (50 μl) diluted at 1:1,000 in the blocking solution were added to the wells and incubated for 1 h at RT. The plates were incubated with 50 μl of biotinylated rat anti-mouse IgG1 or IgG2a diluted at 1:5,000 in blocking solution for 1 h at RT and finally with Sv-HRP diluted at 1:4,000 in blocking solution for 30 min at RT. The plates were washed three to five times with PBS/Tween 20 in between each step. The plates were developed and read as described for the total IgG levels.

Splenocyte Proliferation and IFN-γ Release Assay

The spleens were crushed in 1X Hanks Balanced Salt Solution (HBSS) using a stomacher homogenizer for 60 s at normal speed to obtain single cell suspensions and the suspensions were then transferred into centrifuge tubes. Red blood cells were lysed by adding 1X ammonium chloride/potassium hydrogen carbonate (ACK) buffer (156 mM NH_4Cl, 10 mM $KHCO_3$ and 100 μM EDTA) and incubating for 1–2 min at RT. The cells were spun down at 1,500 rpm, 4°C for 10 min. Supernatants were decanted and the cells were washed two more times with 1X HBSS. The cells were resuspended in RPMI 1640 (supplemented with 10% heat-

inactivated fetal calf serum, 1 mM HEPES, 2 μM l-glutamine, 10 U/ml penicillin, 100 U/ml streptomycin, 50 μM 2-mercaptoethanol). For splenocyte proliferation assay, cells (5×10^5 cells/well) were added to a 96-well plate and incubated with media, Con A (2 μg/ml), or his-tag p24 (1 μg/ml) at 37°C, 7% CO_2 for 4 days. The cells were pulsed with 1 μCi of ^{3}H-thymidine on day 4 and incubated for an additional 24 h at 37°C, 7% CO_2. On day 5, the cells were harvested onto 96-well plates with filters and counted to measure T cell proliferation.

To measure IFN-γ release from stimulated splenocytes, parallel 48-well plates were set up using 1×10^6 cells/well (total volume of 400 μl) and incubated with media alone, Con A (2 μg/ml), or his-tag p24 (1 μg/ml) at 37°C, 7% CO_2 for 72 h. The supernatants were collected at 72 h and stored at −80°C for IFN-γ analysis by ELISA (performed per manufacturer's instructions).

Statistical Analysis

Statistical analysis was performed using one-way analysis of variances (ANOVA) followed by pair-wise comparisons using Tukey's multiple comparison test using GraphPad Prism software.

RESULTS AND DISCUSSION

Preparation of Ni-NPs and Initial *In Vivo* Study with Ni-NPs

NPs prepared using oil-in-water microemulsion precursors have been reported previously (20,42,43). These NPs offer versatility in entrapment of ligands and molecules and can be easily engineered to be neutral, anionic, or cationic based on the appropriate choice of surfactant(s). In these studies, neutral NPs were prepared using non-ionic emulsifying wax as the oil phase and the neutral surfactant Brij 78. To incorporate a small amount of surface-chelated nickel, the use of the lipid DOGS–NTA–Ni (Fig. 1) was explored. The hydrophobic portion of this molecule is thought to be entrapped within the oil phase, exposing the NTA–Ni portion on the surface of the NPs for interaction with histidine-tags on proteins. The Ni-NPs had a mean size of 145.0±5.5 nm with a mean polydispersity index of 0.247±0.040 (n=6) and were slightly negatively charged (−30 to −20 mV). Based on theoretical calculations, these Ni-NPs were initially bound to his-tag p24 at a 1:10 w/w ratio for initial *in vivo* evaluation to determine the applicability of this technology for further development. The binding of his-tag p24 to the Ni-NPs was confirmed by SDS-PAGE (data not shown). The use of DOGS–NTA entrapped in NPs was also investigated to control for non-specific adsorption of the protein on the surface of the NPs. The carboxylic groups of the NTA are thought to give the NPs a net negative charge and could allow his-tag p24, a cationic protein, to be coated on the surface of the particles. As shown in Fig. 2, the Ni-NPs resulted in significant enhancement in antibody responses compared to both Alum and NTA-NPs. These initial studies were very encouraging in that they demonstrated that superior humoral responses could be obtained with these Ni-NPs compared to the conventional coated NPs and Alum.

Ni-NP Formulations Optimized and Characterized with His-tag GFP

Based on the promising results obtained with the initial *in vivo* studies, further work to optimize and characterize the Ni-NPs using his-tag GFP was performed. The use of this protein offered numerous advantages in optimizing the formulations such as ease of detection by fluorescence, direct quantitation of the protein bound to the NPs and released from the NPs. In addition, GFP is similar in molecular weight to his-tag p24, 28 kDa for GFP versus 24 kDa for his-tag p24. Separation of his-tag GFP bound to Ni-NPs from unbound his-tag GFP was achieved by GPC using a Sepharose CL4B column. The eluent from the GPC purification can be fractionated (1 ml) and based on the particle size intensity and fluorescence intensity measurements, NPs and protein associated with NPs were found to elute in fractions 3 to 6, whereas free protein eluted in later fractions, 8 to 12 (Fig. 3). Moreover, during these binding studies, it was discovered that the Ni-NP formulation contained some unentrapped DOGS–NTA–Ni, which could also be separated from the NPs by GPC since it elutes mostly in fractions 7–9 (Fig. 3). Thus, GPC purification with a Sepharose CL4B column allowed efficient separation of the unentrapped lipid from Ni-NPs and for separating unbound his-tag protein from the Ni-NP bound protein. As shown in Fig. 3, the GPC purification of excess lipid from Ni-NPs allowed for higher amount of his-tag protein being bound to the surface of the NPs (purified Ni-NPs shown as solid triangles) and subse-

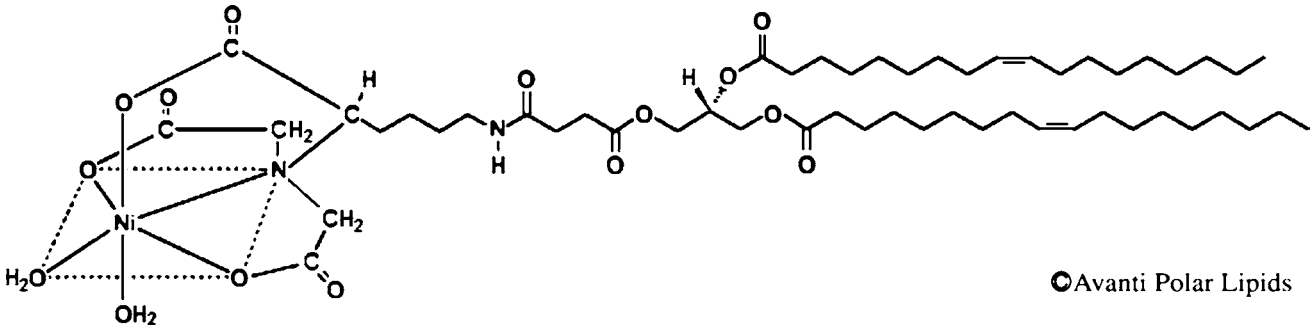

Fig. 1 Structure of DOGS–NTA–Ni. NTA occupies four of the Ni coordination sites, leaving two unoccupied sites (shown coordinating with water in figure) for interaction with the histidine residues. (Structure was copied from Avanti Polar Lipids website: http://www.avantilipids.com/SyntheticNickel-ChelatingLipids.asp).

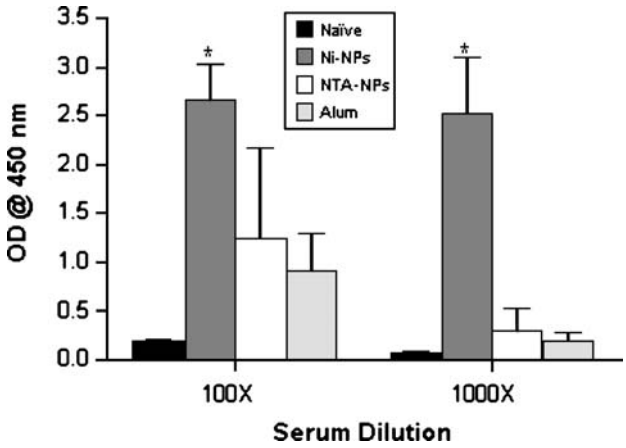

Fig. 2 Gag p24-specific IgG levels in serum at 4 weeks post initial immunization. Mice were immunized with 2.5 μg of his-tag p24 bound to Ni-NPs (25 μg), coated on NTA-NPs (25 μg), or adjuvanted with Alum (25 μg) on day 0 and day 14. Data for each group represents the mean ± SD (n=5–6). *p<0.01 compared to all groups.

quently, GPC purification of NPs was performed prior to reacting with his-tag proteins.

The binding of his-tag GFP with Ni-NPs was evaluated at two ratios and it was found that at a 1:33.7 w/w ratio of his-tag GFP to Ni-NPs, the majority of the protein (>80%) was bound to the surface of the NPs (Fig. 4). Furthermore, to determine the specificity of the binding, GPC purified NTA-NPs were mixed with his-tag GFP and the binding was evaluated. As shown in Fig. 4, very little protein was associated with the NTA-NPs (~7%) and the majority of the protein eluted in later fractions where free protein is expected to elute. These data suggested that the binding to the Ni-NPs was stronger and more specific than simple adsorption on the surface of the particles. The his-tag GFP binding to Ni-NPs was found to be stable for 4 h in PBS at 37°C, pH 7.4 with 12.0±5.0% of the protein released and particle sizes retained at

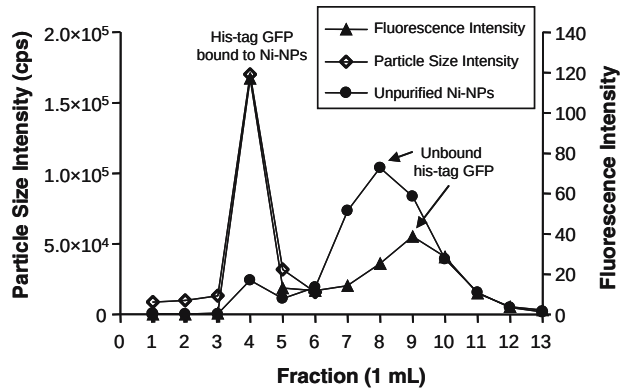

Fig. 3 GPC separation profiles using Sepharose CL4B column. Ni-NPs eluted in fraction 3–6 as determined by particle size intensity. The extent of his-tag GFP bound to Ni-NPs can be determined by separating protein bound to Ni-NPs from free protein, which elutes in faction 8–12 as determined by fluorescence intensity measurements. Fluorescence of the protein when bound to Ni-NPs overlaps with correlating particle size intensities in fraction 3–6. The peak for his-tag GFP bound to excess lipid in the unpurified Ni-NPs shifts to the left, eluting in fraction 7–12, based on fluorescence intensity measurements.

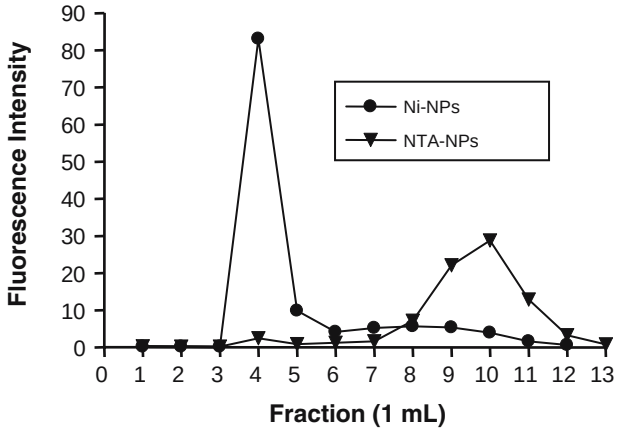

Fig. 4 Binding of his-tag GFP to Ni-NPs compared to NTA-NPs. The GPC purification profile for his-tag GFP bound to Ni-NPs at 1:33.7 w/w ratio of protein to Ni-NPs demonstrated that greater than 80% of the protein was bound to Ni-NPs. At this same ratio, the GPC purification profile for his-tag GFP mixed with NTA-NPs indicated that 7% of the protein was associated with the NTA-NPs.

approximately 160 nm over the time frame. Furthermore, his-tag GFP bound to Ni-NPs at 1:33.7 w/w ratio was stable at 4°C, with only 4.3±2.3% of the protein released after incubating for 7 days in PBS, pH 7.4.

Entrapment Efficiency of DOGS–NTA–Ni in NPs Based on Ni

The amount of DOGS–NTA–Ni entrapped in NPs was calculated indirectly by quantitating the amount of Ni associated with the NPs before and after GPC purification using AES. The molar ratio of Ni chelated with DOGS–NTA was 1:1, therefore the entrapment efficiency of the lipid was calculated based on the Ni. As controls, the amount of Ni present in NTA-NPs was evaluated and the recovery of Ni from this matrix was also determined using NTA-NPs. As expected, no Ni was detected in the control NTA-NP preparations. In addition, the spike-recovery studies suggested that the Ni could be recovered from the NP matrix, with greater than 80% recovery at the highest amount of NPs evaluated (Table I). Based on the amount of Ni associated with NPs before and after GPC purification in four independent Ni-NP preparations, it was calculated that approximately 5% of the lipid used in the initial preparation was entrapped within the NPs (Table II). Furthermore, based on these calculations, it was concluded that there was a 3-fold excess of Ni present on the NPs at the 1:33.7 w/w ratio of his-tag

Table I. Ni Spike and Recovery from NTA-NPs. Spike and Recovery Studies with Ni were Performed at 10 and 50 ppb using 0.4 and 2.0 mg of NTA-NPs

NTA-NPs (n=3) (mg)	Ni Spike (ppb)	Average Ni Recovery (%)	Standard Deviation
0.4	10	102.1	19.0
0.4	50	104.8	1.8
2.0	10	87.8	9.6
2.0	50	89.6	5.1

Table II. Quantitation of Ni on NP Surface Before and After GPC Purification by AES

Ni-NP Preparation	μg Ni Before GPC*	μg Ni After GPC*	Molecules Ni per Particle	Molecules of GFP per Particle	Molar Ratio of GFP to Ni
1	8.19	0.53			
2	7.87	0.38	3,557	1,039	1 to 3
3	7.82	0.27			
4	7.85	0.49			

*Values reflect amount of Ni per 2 mg of NPs

GFP to NPs. Interestingly, increasing the protein to NP ratio from 1:16.9 to 1:33.7 w/w only resulted in a slight increase in binding efficiency from about 70% to 80%. This combined with the fact that there is still a three-fold excess of Ni on the NPs at the higher binding ratio suggests that there may have been some steric hindrance preventing accessibility to at least some of the Ni present on NPs for binding to the protein. Alternatively, it is possible that some of the chelated Ni was entrapped in the oil phase and thus not accessible for binding with the his-tag protein.

Optimized Ni-NP Formulations with His-tag p24

Based on the binding studies for his-tag GFP with Ni-NPs, the optimal binding ratios of his-tag p24 to Ni-NPs was evaluated for further use in *in vivo* studies. Evaluating the binding of his-tag p24 was more challenging because, unlike GFP, it could not be assessed directly on Ni-NPs. To determine the optimal binding ratios, the relative amounts of unbound his-tag p24 were detected using ELISA (Fig. 5A) and the fractions containing Ni-NPs were analyzed for presence of bound his-tag p24 by Western blot (Fig. 5B). Analysis of the Western blot by densitometry suggested that greater than 80% of the protein was associated with the Ni-NPs at ratios higher than 1:35.4 w/w. Thus, for further *in vivo* evaluation the 1:35.4 w/w ratio was used to prepare the formulation with Ni-NPs and with control NTA-NPs.

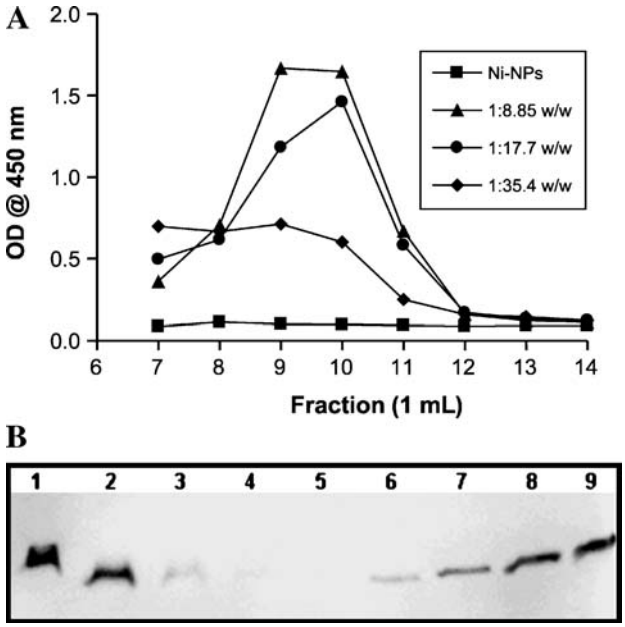

Fig. 5 Binding of his-tag p24 to Ni-NPs. (A) GPC profile for free his-tag p24 eluting from column. His-tag p24 was bound to Ni-NPs at various ratios and the relative amounts of free protein eluting from the Sepharose CL4B GPC column were traced in the fractions where free protein is expected to elute using ELISA. Ni-NPs with no protein were run as control with the ELISA to account for any interference. (B) Western blot of his-tag p24 bound to Ni-NPs. Fractions 3–5 from the GPC purification were collected, combined, and analyzed by western blot to determine the relative amounts of his-tag p24 bound to the Ni-NPs. The lanes correspond to the following samples: (1) 1:70.8 w/w; (2) 1:35.4 w/w; (3) 1:17.7 w/w; (4) 1:8.85 w/w; (5) Ni-NPs as control; 6–9 are 50, 100, 200, and 250 ng of his-tag p24 standards loaded at controls, respectively. Greater than 80% of the his-tag p24 was bound to the Ni-NPs at ratios greater than 1:35.4 w/w.

In Vitro Release of His-tag p24 from Ni-NPs as a Function of pH

Figure 6 shows that lowering the pH resulted in a reduction in the relative amount of his-tag p24 bound to the Ni-NPs after 1 h. Specifically, at a pH of 5 and below, there were negligible amounts of his-tag p24 remaining associated with the NPs, as expected. Based on these studies, the his-tag protein is expected to remain associated with the Ni-NPs to a significant extent until being taken up into the cells and exposed to the acidic environment of the endosomes or

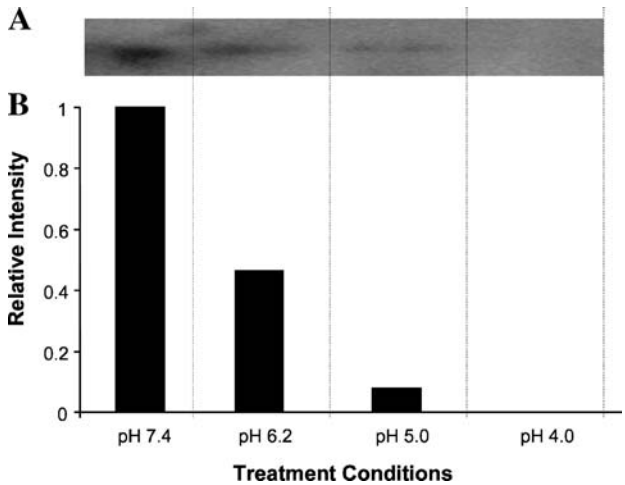

Fig. 6 Release of his-tag p24 from Ni-NPs as a function of pH. (A) Western blot of his-tag p24 retained on nanoparticles incubated at different pHs. His-tag p24 bound to Ni-NPs were incubated for 1 h at pH 7.4, 6.2, 5.0 and 4.0 at 25°C. Ni-NPs were then separated from free his-tag protein by GPC after which they were concentrated and run on SDS-PAGE. (B) Densitometry analysis of the western blot using Kodak 1D software. The amount of his-tag p24 retained on the Ni-NPs under different pHs was determined by quantifying the intensities of the bands relative to that of the control (pH 7.4). The amount of released his-tag p24 was not quantified.

lysosomes, where release of his-tag p24 from the Ni-NPs most likely occurs. Thus, it is probable that a greater amount of the his-tag protein accumulates in the cell with the Ni-NPs compared to charged NPs, leading to stronger immune responses *in vivo*. However, it is unclear that the his-tag p24 needs to be released from the Ni-NPs to result in an immune response since theoretically the lysosomal environment is well-equipped to digest intact particulate pathogens and subsequently allow for the processing and presentation of the protein antigen.

In Vivo Results Using Optimized Ni-NP Formulations with His-tag p24

Initial *in vivo* studies demonstrated the potential of Ni-NPs for enhancing humoral immune responses to his-tag p24. However, these formulations were not optimized and some of the protein could have been associated with excess, unentrapped lipid instead of NPs, leading to suboptimal *in vivo* responses. The goal of this follow up *in vivo* study was to confirm that humoral immune responses could be obtained

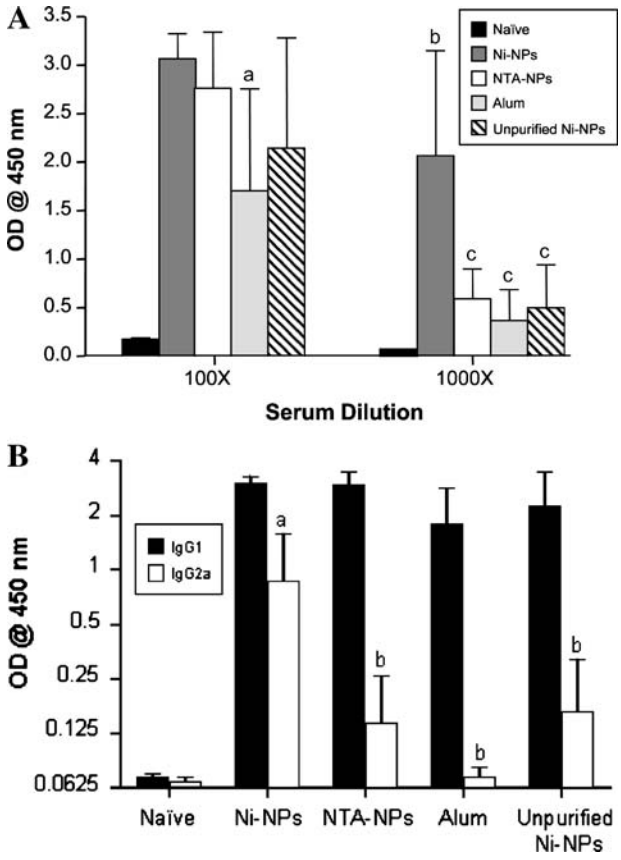

Fig. 7 His-tag p24-specific humoral responses after immunization with optimized Ni-NP formulations. Mice were immunized with 2.5 μg of his-tag p24 bound to Ni-NPs (88.5 μg), coated on NTA-NPs (88.5 μg), adjuvanted with Alum (88.5 μg) or mixed with unpurified Ni-NPs (88.5 μg) on day 0 and day 14. (A) Total serum IgG levels were measured on day 28. Data for each group represents the mean ± SD (n=6–8). [a]p<0.01 compared to Ni-NP group; [b]p<0.001 compared to all groups; [c]p>0.05 compared to naïve group. (B) Serum IgG1 and IgG2a levels were measured on day 28 by ELISA at a 1:1,000 serum dilution. Data for each group represents the mean ± SD (n=6–8). [a]p<0.001 compared to all groups; [b]p>0.05 compared to naïve group.

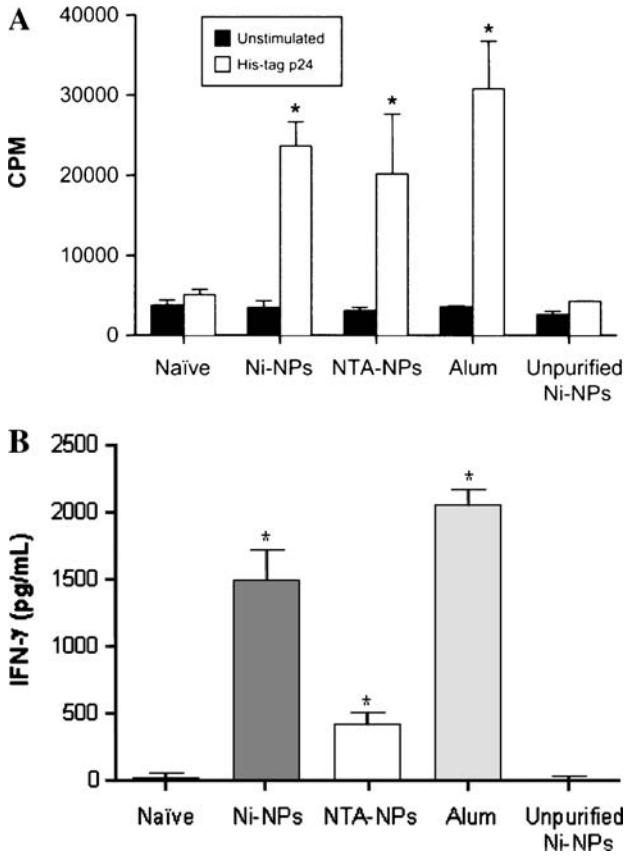

Fig. 8 Cellular responses to his-tag p24. Mice were immunized with 2.5 μg of his-tag p24 on day 0 and day 14. Spleens were harvested and pooled for each group on day 28. (A) Splenocyte proliferation results. Cells (5×10^5) were stimulated with 1 μg/ml his-tag p24 and the incorporation of ^{3}H-thymidine in cells was evaluated on day 5. The data represents the mean ± SD (n=3). *p<0.05 compared to unstimulated cells. (B) 72 h IFN-γ release from stimulated splenocytes. Cells (1×10^6) were stimulated with 1 μg/ml his-tag p24 and the supernatants were evaluated for IFN-γ release at 72 h by ELISA. The data represents the mean ± SD (n=3). *p<0.05 compared to unstimulated cells.

with the optimized formulations of Ni-NPs and to further evaluate the cellular immune responses. Mice were immunized with his-tag p24 bound to Ni-NPs, coated on control NTA-NPs or adjuvanted with Alum. In addition, to control for the immune responses that may have been enhanced by unentrapped lipid bound to his-tag p24, the use of unpurified Ni-NPs was also investigated. At the 1:1,000 serum dilution, significantly higher his-tag p24-specific IgG levels were detected using the Ni-NPs compared to all groups (Fig. 7A). Moreover, NTA-NPs, Alum, and unpurified Ni-NP groups were statistically insignificant compared to the naïve group. Interestingly, the unpurified Ni-NPs demonstrated similar potency in generating antibodies as the NTA-NPs and Alum, but significantly less compared to the purified Ni-NPs. It is hypothesized that his-tag p24 would interact with unentrapped lipid, which exists freely in solution, in micelles, or loosely adsorbed on the NP surface, to a greater extent because the Ni would be more accessible for interactions compared to the Ni-chelated to lipid which is entrapped in the NPs. Thus, while there may be some enhancement in

antigen uptake and subsequently antibody production with the unpurified Ni-NP formulation, the results demonstrate that they are only marginal compared to the responses that can be generated with the antigen being bound to the Ni on the NPs. Moreover, this data supports that protein bound to Ni-NPs is superior to Alum and NTA-NPs in enhancing humoral immune responses to his-tag p24.

The serum isotype levels, IgG1 versus IgG2a, were measured to assess the type of immune response generated (i.e., Th1 or Th2). During an immune response, the release of Th1 or Th2 cytokines will affect the production of these antibodies. BALB/c mice bias the immune response towards a Th2 profile (44,45), generating antibodies of IgG1 isotype; however, in the presence of Th1 type immune responses, the cells produce IFN-γ which causes a switch in the isotype produced to IgG2a. The isotype analysis in these studies revealed that the Ni-NPs resulted in the highest levels of IgG2a compared to all groups, while the IgG1 levels were comparable to the other three immunized groups (Fig. 7B).

The cellular immune responses in these studies were evaluated by splenocyte proliferation and IFN-γ release assays. Splenocytes from immunized mice that were stimulated *in vitro* with his-tag p24 demonstrated significantly higher proliferation with all groups compared to naïve group, with the exception of the unpurified Ni-NPs group (Fig. 8A). In addition, the IFN-γ released from the stimulated splenocytes showed a similar trend in that all groups, except the unpurified Ni-NPs, produced significantly higher IFN-γ compared to the naïve group (Fig. 8B). However, the IFN-γ release was only modest with both the Ni-NP and Alum groups (cytokine levels in the picogram per milliliter range). It is interesting to note that although weak antibody responses could be generated with the unpurified Ni-NPs, they were not effective at inducing his-tag p24-specific cellular responses, as indicated in the splenocyte proliferation and IFN-γ release assays. This could be due to very little antigen actually being bound to the Ni on the NPs because of binding to the more accessible unentrapped lipid, as discussed above. Alternatively, the dose of DOGS–NTA–Ni given with these NPs is higher that that of the purified Ni-NPs and could have an affect on the immune responses. Therefore, further assessment of various doses of Ni-NPs would be beneficial in elucidating the effect of Ni on the immune responses and the optimal doses for enhancing both cellular and humoral immune responses. It is important to note that based on the AES characterization of Ni-NPs, the dose of Ni administered to mice in each 100 μl injection in the purified Ni-NPs is equivalent to 20 ng. This amount of Ni is approximately 10,000-fold lower than the levels of Ni that have shown adverse effects in mice (46,47). To provide additional perspective, the average human diet is estimated to contain 0.15 mg Ni per day and drinking water alone contains 0.001 to 0.01 mg Ni per Liter (48). Thus, the dose of Ni used in these studies is considered to be within the tolerable range.

CONCLUSIONS

In conclusion, the preparation of novel NPs containing a small amount of surface-chelated nickel was shown to be effective for enhancing the interaction with his-tag proteins compared to simple charged particles. This stronger affinity of the antigen for the Ni-NPs resulted in superior humoral immune responses *in vivo* compared to protein adjuvanted with Alum or coated on charged NPs. Moreover, the Ni-NPs are also promising for generating Th1 type immune responses. These data demonstrate the potential applications of Ni-NPs for vaccine delivery and warrant further investigation of these systems for enhancing immune responses with protein-based vaccines.

ACKNOWLEDGMENTS

This research was funded by NIH-NIAID AI058842 to RJM and JGW. J. Patel was supported, in part, by a Predoctoral fellowship received from the American Foundation for Pharmaceutical Education and the 2005 Dissertation Year Fellowship received from the University of Kentucky Graduate School. The authors would like to thank Tricia Coakley in the Environmental Research and Training Laboratory (ERTL) at the University of Kentucky for her technical assistance in analyzing nanoparticle samples by AES.

REFERENCES

1. R. K. Gupta and G. R. Siber. Adjuvants for human vaccines—current status, problems and future prospects. *Vaccine* **13**:1263–1276 (1995).
2. J. R. Pink and M. P. Kieny. 4th meeting on novel adjuvants currently in/close to human clinical testing world health organization—organisation Mondiale de la Sante Fondation Merieux, Annecy, France, 23–25, June 2003. *Vaccine* **22**:2097–2102 (2004).
3. M. Singh and D. T. O'Hagan. Recent advances in vaccine adjuvants. *Pharm. Res.* **19**:715–728 (2002).
4. D. T. O'Hagan and M. Singh. Microparticles as vaccine adjuvants and delivery systems. *Expert Rev. Vaccines* **2**:269–283 (2003).
5. W. Jiang, R. K. Gupta, M. C. Deshpande, and S. P. Schwendeman. Biodegradable poly(lactic-co-glycolic acid) microparticles for injectable delivery of vaccine antigens. *Adv. Drug Deliv. Rev.* **57**:391–410 (2005).
6. G. F. Kersten and D. J. Crommelin. Liposomes and ISCOMs. *Vaccine* **21**:915–920 (2003).
7. A. G. Coombes, E. C. Lavelle, P. G. Jenkins, and S. S. Davis. Single dose, polymeric, microparticle-based vaccines: the influence of formulation conditions on the magnitude and duration of the immune response to a protein antigen. *Vaccine* **14**:1429–1438 (1996).
8. R. K. Gupta, M. Singh, and D. T. O'Hagan. Poly(lactide-co-glycolide) microparticles for the development of single-dose controlled-release vaccines. *Adv. Drug Deliv. Rev.* **32**:225–246 (1998).
9. A. I. Bot, D. J. Smith, S. Bot, L. Dellamary, T. E. Tarara, S. Harders, W. Phillips, J. G. Weers, and C. M. Woods. Receptor-mediated targeting of spray-dried lipid particles coformulated with immunoglobulin and loaded with a prototype vaccine. *Pharm. Res.* **18**:971–979 (2001).
10. M. Sugimoto, K. Ohishi, M. Fukasawa, K. Shikata, H. Kawai, H. Itakura, M. Hatanaka, R. Sakakibara, M. Ishiguro, M. Nakata, et al. Oligomannose-coated liposomes as an adjuvant for the induction of cell-mediated immunity. *FEBS Lett.* **363**:53–56 (1995).
11. H. Xie, I. Gursel, B. E. Ivins, M. Singh, D. T. O'Hagan, J. B. Ulmer, and D. M. Klinman. CpG oligodeoxynucleotides adsorbed onto polylactide-co-glycolide microparticles improve the immunogenicity and protective activity of the licensed anthrax vaccine. *Infect. Immun.* **73**:828–833 (2005).

12. J. Kazzaz, M. Singh, M. Ugozzoli, J. Chesko, E. Soenawan, and D. T. O'Hagan. Encapsulation of the immune potentiators MPL and RC529 in PLG microparticles enhances their potency. *J. Control Release* **110**:566–573 (2006).
13. D. T. O'Hagan, M. L. MacKichan, and M. Singh. Recent developments in adjuvants for vaccines against infectious diseases. *Biomol. Eng.* **18**:69–85 (2001).
14. A. Moore, P. McGuirk, S. Adams, W. C. Jones, J. P. McGee, D. T. O'Hagan, and K. H. Mills. Immunization with a soluble recombinant HIV protein entrapped in biodegradable microparticles induces HIV-specific CD8 cytotoxic T lymphocytes and CD4 Th1 cells. *Vaccine* **13**:1741–1749 (1995).
15. A. M. Carcaboso, R. M. Hernandez, M. Igartua, J. E. Rosas, M. E. Patarroyo, and J. L. Pedraz. Potent, long lasting systemic antibody levels and mixed Th1/Th2 immune response after nasal immunization with malaria antigen loaded PLGA microparticles. *Vaccine* **22**:1423–1432 (2004).
16. M. Singh, J. Chesko, J. Kazzaz, M. Ugozzoli, E. Kan, I. Srivastava, and D. T. O'Hagan. Adsorption of a novel recombinant glycoprotein from HIV (Env gp120dV2 SF162) to anionic PLG microparticles retains the structural integrity of the protein, whereas encapsulation in PLG microparticles does not. *Pharm. Res.* **21**:2148–2152 (2004).
17. D. T. O'Hagan. Microparticles and polymers for the mucosal delivery of vaccines. *Adv. Drug Deliv. Rev.* **34**:305–320 (1998).
18. A. Debin, R. Kravtzoff, J. V. Santiago, L. Cazales, S. Sperandio, K. Melber, Z. Janowicz, D. Betbeder, and M. Moynier. Intranasal immunization with recombinant antigens associated with new cationic particles induces strong mucosal as well as systemic antibody and CTL responses. *Vaccine* **20**:2752–2763 (2002).
19. M. Singh, J. Kazzaz, M. Ugozzoli, J. Chesko, and D. T. O'Hagan. Charged polylactide co-glycolide microparticles as antigen delivery systems. *Expert. Opin. Biol. Ther.* **4**:483–491 (2004).
20. Z. Cui and R. J. Mumper. Coating of cationized protein on engineered nanoparticles results in enhanced immune responses. *Int. J. Pharm.* **238**:229–239 (2002).
21. Z. Cui, J. Patel, M. Tuzova, P. Ray, R. Phillips, J. G. Woodward, A. Nath, and R. J. Mumper. Strong T cell type-1 immune responses to HIV-1 Tat (1–72) protein-coated nanoparticles. *Vaccine* **22**:2631–2640 (2004).
22. J. Patel, D. Galey, J. Jones, P. Ray, J. G. Woodward, A. Nath, and R. J. Mumper. HIV-1 Tat-coated nanoparticles result in enhanced humoral immune responses and neutralizing antibodies compared to alum adjuvant. *Vaccine* **24**:3564–3573 (2006).
23. P. Elamanchili, M. Diwan, and M. Cao. Characterization of poly(D,L-lactic-co-glycolic acid) based nanoparticulate system for enhanced delivery of antigens to dendritic cells. *Vaccine* **22**:2406–2412 (2004).
24. M. E. Lutsiak, D. R. Robinson, C. Coester, G. S. Kwon, and J. Samuel. Analysis of poly(D,L-lactic-co-glycolic acid) nanosphere uptake by human dendritic cells and macrophages in vitro. *Pharm. Res.* **19**:1480–1487 (2002).
25. H. Sun, K. G. Pollock, and J. M. Brewer. Analysis of the role of vaccine adjuvants in modulating dendritic cell activation and antigen presentation *in vitro*. *Vaccine* **21**:849–855 (2003).
26. V. Weissig, J. Lasch, A. L. Klibanov, and V. P. Torchilin. A new hydrophobic anchor for the attachment of proteins to liposomal membranes. *FEBS Lett.* **202**:86–90 (1986).
27. V. P. Torchilin, T. S. Levchenko, A. N. Lukyanov, B. A. Khaw, A. L. Klibanov, R. Rammohan, G. P. Samokhin, and K. R. Whiteman. p-Nitrophenylcarbonyl-PEG-PE-liposomes: fast and simple attachment of specific ligands, including monoclonal antibodies, to distal ends of PEG chains via p-nitrophenylcarbonyl groups. *Biochim. Biophys. Acta* **1511**:397–411 (2001).
28. T. D. Heath and F. J. Martin. The development and application of protein–liposome conjugation techniques. *Chem. Phys. Lipids* **40**:347–358 (1986).
29. J. Crowe, B. S. Masone, and J. Ribbe. One-step purification of recombinant proteins with the 6xHis tag and Ni–NTA resin. *Methods Mol. Biol.* **58**:491–510 (1996).
30. J. Porath, J. Carlsson, I. Olsson, and G. Belfrage. Metal chelate affinity chromatography, a new approach to protein fractionation. *Nature* **258**:598–599 (1975).
31. E. Hochuli, H. Dobeli, and A. Schacher. New metal chelate adsorbent selective for proteins and peptides containing neighbouring histidine residues. *J. Chromatogr.* **411**:177–184 (1987).
32. J. Schmitt, H. Hess, and H. G. Stunnenberg. Affinity purification of histidine-tagged proteins. *Mol. Biol. Rep.* **18**:223–230 (1993).
33. S. A. Lauer and J. P. Nolan. Development and characterization of Ni–NTA-bearing microspheres. *Cytometry* **48**:136–145 (2002).
34. H. Celia, E. Wilson-Kubalek, R. A. Milligan, and L. Teyton. Structure and function of a membrane-bound murine MHC class I molecule. *Proc. Natl. Acad. Sci. USA* **96**:5634–5639 (1999).
35. G. G. Chikh, W. M. Li, M. P. Schutze-Redelmeier, J. C. Meunier, and M. B. Bally. Attaching histidine-tagged peptides and proteins to lipid-based carriers through use of metal-ion-chelating lipids. *Biochim. Biophys. Acta.* **1567**:204–212 (2002).
36. C. L. Broekhovenvan, C. R. Parish, C. Demangel, W. J. Britton, and J. G. Altin. Targeting dendritic cells with antigen-containing liposomes: a highly effective procedure for induction of antitumor immunity and for tumor immunotherapy. *Cancer Res.* **64**:4357–4365 (2004).
37. E. O. Freed. HIV-1 gag proteins: diverse functions in the virus life cycle. *Virology* **251**:1–15 (1998).
38. F. Buseyne, M. McChesney, F. Porrot, S. Kovarik, B. Guy, and Y. Riviere. Gag-specific cytotoxic T lymphocytes from human immunodeficiency virus type 1-infected individuals: Gag epi topes are clustered in three regions of the p24gag protein. *J. Virol.* **67**:694–702 (1993).
39. J. Kazzaz, J. Neidleman, M. Singh, G. Ott, and D. T. O'Hagan. Novel anionic microparticles are a potent adjuvant for the induction of cytotoxic T lymphocytes against recombinant p55 gag from HIV-1. *J. Control Release* **67**:347–356 (2000).
40. V. Novitsky, H. Cao, N. Rybak, P. Gilbert, M. F. McLane, S. Gaolekwe, T. Peter, I. Thior, T. Ndung'u, R. Marlink, T. H. Lee, and M. Essex. Magnitude and frequency of cytotoxic T-lymphocyte responses: identification of immunodominant regions of human immunodeficiency virus type 1 subtype C. *J. Virol.* **76**:10155–10168 (2002).
41. R. Zuniga, A. Lucchetti, P. Galvan, S. Sanchez, C. Sanchez, A. Hernandez, H. Sanchez, N. Frahm, C. H. Linde, H. S. Hewitt, W. Hildebrand, M. Altfeld, T. M. Allen, B. D. Walker, B. T. Korber, T. Leitner, J. Sanchez, and C. Brander. Relative dominance of Gag p24-specific cytotoxic T lymphocytes is associated with human immunodeficiency virus control. *J. Virol.* **80**:3122–3125 (2006).
42. M. O. Oyewumi and R. J. Mumper. Gadolinium-loaded nanoparticles engineered from microemulsion templates. *Drug Dev. Ind. Pharm.* **28**:317–328 (2002).
43. Z. Cui and R. J. Mumper. Genetic immunization using nanoparticles engineered from microemulsion precursors. *Pharm. Res.* **19**:939–946 (2002).
44. M. L. Guler, N. G. Jacobson, U. Gubler, and K. M. Murphy. T cell genetic background determines maintenance of IL-12 signaling: effects on BALB/c and B10.D2 T helper cell type 1 phenotype development. *J. Immunol.* **159**:1767–1774 (1997).
45. M. Bix, Z. E. Wang, B. Thiel, N. J. Schork, and R. M. Locksley. Genetic regulation of commitment to interleukin 4 production by a CD4() T cell-intrinsic mechanism. *J. Exp. Med.* **188**: 2289–2299 (1998).
46. J. A. Graham, F. J. Miller, M. J. Daniels, E. A. Payne, and D. E. Gardner. Influence of cadmium, nickel, and chromium on primary immunity in mice. *Environ. Res.* **16**:77–87 (1978).
47. R. J. Smialowicz, R. R. Rogers, M. M. Riddle, and G. A. Stott. Immunologic effects of nickel: I. Suppression of cellular and humoral immunity. *Environ. Res.* **33**:413–427 (1984).
48. NPER Association and ND Institute. *Safe Use of Nickel in the Workplace*. Nickel Development Institute and Nickel Producers Environmental Research Association, Durham, North Carolina, 1997.